Novel cooling system for free-standing photovoltaic panels

Mahyar Kargaran[a], Hamid Reza Goshayeshi[a], Seyed Reza Saleh[a], Iman Zahmatkesh[a], and Issa Chaer[b]

[a]Department of Mechanical Engineering, Mashhad Branch, Islamic Azad University, Mashhad, Iran; [b]School of Built Environment and Architecture, London South Bank University, London, UK

ABSTRACT

Although photovoltaic (PV) technologies enjoy tremendous benefits and hold the huge potential to lower building overall energy consumption, there is a major drawback. PV efficiency is extremely sensitive to heat and significantly reduced by increasing setting temperature and solar irradiance; thereby, thermal management in PV collectors plays a significant role in generating electrical energy. Using oscillating heat pipes attached to the rear side of PV panels is considered a novel and useful approach to dissipating heat. In this study, a novel cooling system that consists of a newly designed spiral oscillating heat pipe is introduced, while DI water and 0.2 g/l graphene are used as working fluid and PV panels are located at tilt angles of 30° and 60°. The OHP efficiency is higher at 60°; however, the efficiency of PV is maximized at 30° since the panel is exposed to maximum solar irradiance. The research demonstrates that the cooling method proves highly effective, especially in the hottest time of the day and the power output improves considerably from 38 W to more than 42 W at 30°, while the value is about 39.7 W when water is used as a coolant.

Introduction

From 1990 to 2020, energy use rose dramatically, reaching 14,300 million tonnes of oil equivalent (Coldrick et al. 2023b) which has done irreparable damage to the environment and led to climate change as well (Gyamfi, Kwakwa, and Adebayo 2023). On the other hand, the marked increase in the price of conventional sources of energy gave rise to interest in long-lasting and renewable energy sources, and it has grown dramatically. Solar energy is one of the most reliable, cost-effective, and available forms of green energy sources (Tiwari et al. 2023). Photovoltaic technology is a pragmatic approach to harnessing solar energy (Hamid et al. 2023). PV electrical energy ranges between 5% and 25% (Browne, Norton, and McCormack 2016), and it is crucial to promote panel efficiency to fulfill energy demand. Low operational and maintenance costs are considered overwhelming advantages of PV in comparison with other sources, and recent energy production has exceeded more than 1 TWh in 2022 (Coldrick et al. 2023a). However, PV efficiency seems acutely vulnerable to ambient temperature, which means the efficiency experiences a reduction about 0.5% with an increase in PV cell temperature of 1°C (Divitini et al. 2016). Therefore, to promote PV efficiency, generated heat should be removed. A plethora of methods are utilized to cool down the PV cell temperature, and the most common ones are listed in Figure 1. Given the growing interest in semiconductor concerning thermal management, a heat pipe as a convenient device which has a simple structure and quite efficient has been widely used in cooling industries. This two-phase passive heat transfer device typically comprises a sealed tube divided into three parts, evaporator, condenser, and adiabatic. The section which absorbs heat is known as an evaporator, the area that dissipates heat is called a condenser section, and part of the tube

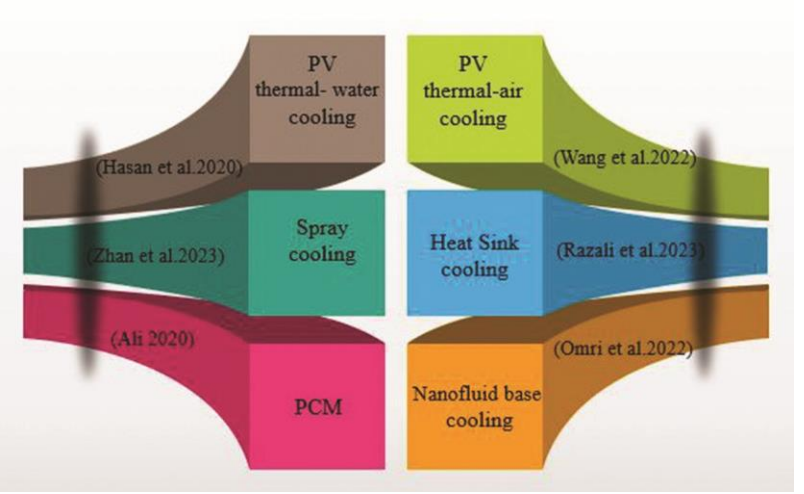

Figure 1. Different major cooling techniques of PV.

between the evaporator and condenser is named an adiabatic section (Zamanifard et al. 2023). The heat pipe is divided into five types (shown in Figure 2 (Jose and Hotta 2023)), which offers high performance in terms of heat transfer (Wang et al. 2022). Being lightweight, cost-effective operation, long-term durability, and simple structure are distinct advantages of heat pipe applications (Alshukri et al. 2022). Heat pipe performance is vulnerable to some factors, such as heat load (Pagliarini, Iwata, and Bozzoli 2023), filling ratio (Ahmadian-Elmi et al. 2023), inner diameter of the tubes (Su et al. 2022), number of twists (Alqahtani et al. 2022), inclination angle (Li et al. 2022), and length of adiabatic, condenser, and evaporator sections (Zhan et al. 2023). Rittidech, Donmaung, and

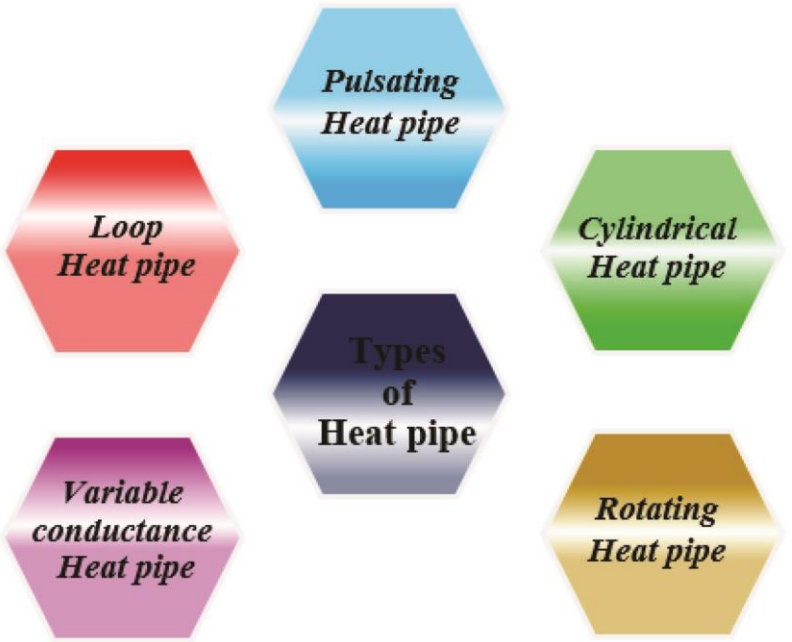

Figure 2. Different types of heat pipes.

Kumsombut (2009) conducted an experimental investigation on the performance of a solar collector joint with an oscillating heat pipe while R134a was used as a coolant. It was demonstrated that not only the system proved highly resistant to corrosion and freezing, but also showed higher energy and economic efficiency.

An oscillating heat pipe (OHP) also known as a pulsating heat pipe (PHP) is rather a new type of heat pipe (Qian et al. 2023) with the capability to handle high heat flux, a lightweight, simple, and flexible structure, which has attracted considerable interest (Salarnia et al. 2023). It comprises a capillary tube bent in several turns (Li et al. 2023). A great number of studies have been conducted to understand a heat transfer mechanism in OHP, and it was observed that the flow pattern and fluid motion have played a significant role in improving thermal performance (Natsume et al. 2011). Concerning flow regime, bubbly, slug, and annular flow proved to be generated one after another when heat load increased (Liu et al. 2019). On the other hand, it has been observed that adding nanoparticles made a significant contribution to enhancing the thermal conductivity of the working fluid, thereby, heat transfer is greatly facilitated (Tawfik 2017). Oscillating heat pipes also deliver impressive performance when nanofluids are used as working fluid (Kargaran et al. 2022). Kaya et al (2019) performed an experimental study on a solar collector integrated with a heat pipe when methanol and CuO-methanol were used as coolants. The thermal collector efficiency with nanofluid reached over 9%. Allouhi and Benzakour Amine (2021) also carried out numerical investigations on cooling solar collection by heat pipe with three different nanofluids (CuO, Al_2O_3, and TiO_2) while the heat pipe with CuO-based nanofluid showed the highest efficiency, 2.7% compared to water. Thanks to the unique features of graphene oxide (GO), such as much higher thermal conductivity compared to copper and aluminum (Huang et al. 2021), lower corrosion in comparison with other nanofluids, higher stability, and lower pressure drops (Sadeghinezhad et al. 2016), it has gained growing popularity since its discovery made in 2004 that is widely used. There are decisive advantages of using graphene oxide, namely, improving thermal conductivity and viscosity of the base fluid and start-up performance of OHP (Novoselov, Blake, and Katsnelson 2008); however, there is a drawback of using a high concentration of graphene oxide nanofluid which can impair thermal process due to its high dynamic viscosity (Nazari et al. 2018). Although a great number of attempts have been made to enhance PV's efficiency, the challenge has yet to be addressed. Although a lot of investigations have been conducted on 2D modules, the investigations being carried out on 3D modules concerned with commercial purposes are very limited. On the other hand, conventional OHP is unable to fulfill demand in the face of the situation when high uniform temperature and high heat flux are required 3D-OHP can be considered as a viable and practical solution to meet the aforementioned requirements (Dai et al. 2024). Qu, Zhao, and Rao (2017) bent two-dimensional OHP into multilayer 3D- OHP. It was observed that 4-layer OHP provided better start-up and heat transfer performance. Lan (2020) designed a new 3D-OHP by manufacturing a closely spaced annular parallel channel, which effectively enhanced the thermal performance of the OHP. He et al (2020) conducted experimental study on the flow pattern and performance of the annular 3D-OHP. An increase in heat input reduced the start-up time and the thermal resistance of the OHP.

The literature analysis indicates a general lack of experimental study concerning the optimization of solar panels' efficiency with 3D-OHP, and either the existing research studies are about just 2D-OHP. Thereby, in this investigation, modeling of solar panels with novel 3D-OHP with different coolants was conducted by experimental data, and the optimal value of the system is considered to achieve the highest electrical efficiency. The object of this research is to propose a new 3D -OHP module which is not only practical for real applications but also increases the applied heat flux as compared to the existing studies. Therefore, at first, the system has been tested at 30° title angle which is the best angle for PV collectors in Mashhad (location of experiment) (Rouhani et al. 2017). And since, it has been shown by Li, Li, and Xu (2019) and Li et al (2019) that around 60°, the heat pipe offers optimum thermal performance, experiments have been conducted at 60°, as well. This study is remarkable and has promising results thanks to its simple and unique structure of OHP, and it offers a highly effective and

cost-effective cooling method to mitigate the PV module temperature. Furthermore, as far as the advantage of proposed system concerns, heat is dissipated from the PV module by a simple and efficient method without external power supply and special maintenance and also easy to install. This newly designed heat pipe enjoys the benefits of 3D-OHP and nanofluids technology and is able to make the most use of solar energy.

Experimental procedure

This section offers a detailed description regarding the test rig and equations employed for the calculations of the results align with error analysis.

Experimental setup

All the tests have been performed in Mashhad, Iran (latitude: 59.6067° E; longitude 36.2972° N) from 24 to 30 August. It should mention that in this study two monocrystalline PV panels (RestarSolar) were used, one of them was considered as the cooled panel equipped with a newly designed three-dimensional OHP and the other reference panel. Table 1 displays the specifications of PV.

As shown in Figure 3, the novel 3D-OHP was designed and fabricated with the red copper tube with the thickness of 1 mm, featured in Figure 4.

It has proved that OHP delivered optimum performance on 50% filling ratio (Alizadeh Jajarm, Goshayeshi, and Bashirnezhad 2022), thereby all the experiments were performed on 50% filling ratio. A vacuum pump, which produces vacuum, was integrated to a valve and the OHP was put under the suction pressure for 15 min. Thereafter, working fluid was injected. The experimental test bed and schematic of test bed are also showed in Figures 5 and 6, respectively.

The steps, which are taken to conduct the study (shown in Figure 7), include using GO and DI water as coolant in two different title angles (30° and 60°).

It is worth mentioning that the lamination technique in order to make a connection between the evaporator section and the back of PV has been used (Aste, Leonforte, and Del Pero 2015); nevertheless, when it comes to the experimental stage, the aforementioned approach was considered to be high-priced and demanding to operate; thereby, a sheet of copper with the thickness of 0.4 mm by means of CPU grease, which has a high thermal conductivity, was attached to the back of PV. Concerning working fluid, the performance of graphene oxide (GO) nanoparticles and distilled water with a concentration of 0.2 gr/lit were investigated. The GO used in this study was purchased from US Research Nanomaterials, Inc. with the purity around 99%. To prepare nanofluid, graphene oxide was prepared by dispersing GO nanoparticles into DI water as a base fluid. As it was mentioned earlier, Nanofluids improve the overall thermal conductivity and heat transfer rate of the base fluid. On the other hand, they should be stable and durable. Since GO nanofluid with surfactant sodium dodecyl sulfate (SDS) proved great stability (Afsari et al. 2023), SDS was also used with a 1:1 ratio. After completing the preparation of working fluid, it is injected into a heat pipe at 50% filling ratio. The FESEM image of graphene oxide is depicted in Figure 8.

The crystal structure of graphene oxide was also assessed by an X-ray diffractometer (XRD), which is shown in Figure 9.

Table 1. Electrical specifications of the PV panel.

Specification	Value
Model number	RTM050M
Nominal maximum power	50 W
Open circuit voltage (V_{OC})	24.6 V
Short circuit current (I_{sc})	2.75 A
Peak voltage (V_{mp})	20 V
Peak current (I_{mp})	2.5 A
Dimension	680 × 547 × 30 mm
η_e	0.134

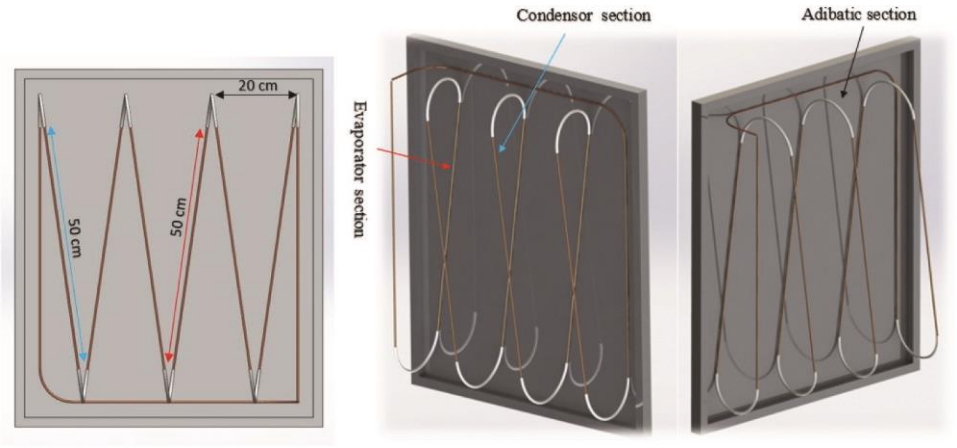

Figure 3. Configuration of newly designed 3D-OHP from different views.

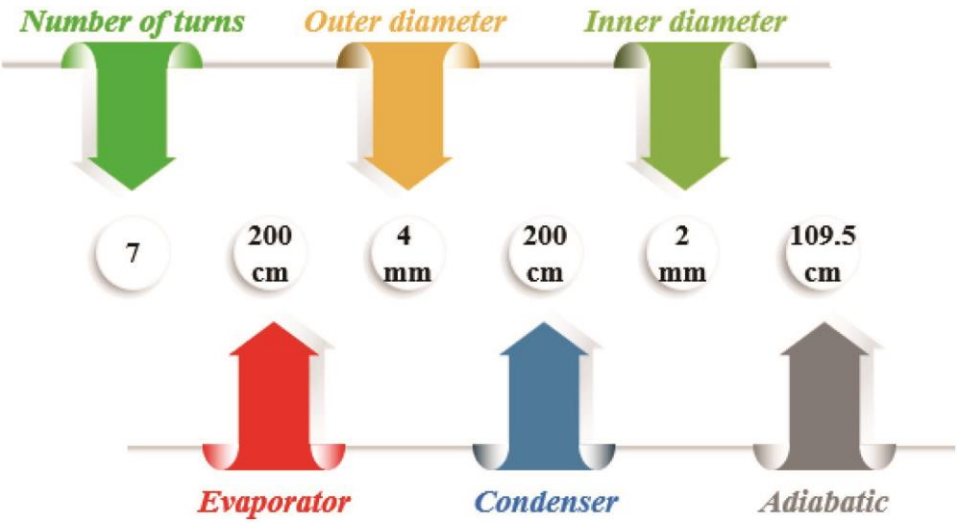

Figure 4. Design parameters of 3D-OHP.

Technical parameters of graphene oxide used in this study are also presented in Table 2.

Tables 3 illustrates thermal conductivity of DI/water and graphene oxide nanofluid with three different concentrations used in this investigation.

Energy analysis

In this part, the formulas applied to conduct energy analysis for OHP-PV are provided.

Temperatures were measured by placing six thermocouples on evaporation and condensation sections, three thermocouples for each section. Thermocouples were attached to temperature data logger BTM-4208SD and when temperatures in evaporation and condensation of the OHP were stabilized, they were recorded and averaged, which means:

$$T_e = \frac{1}{4}\sum_{i=1}^{4} T_i \quad (1)$$

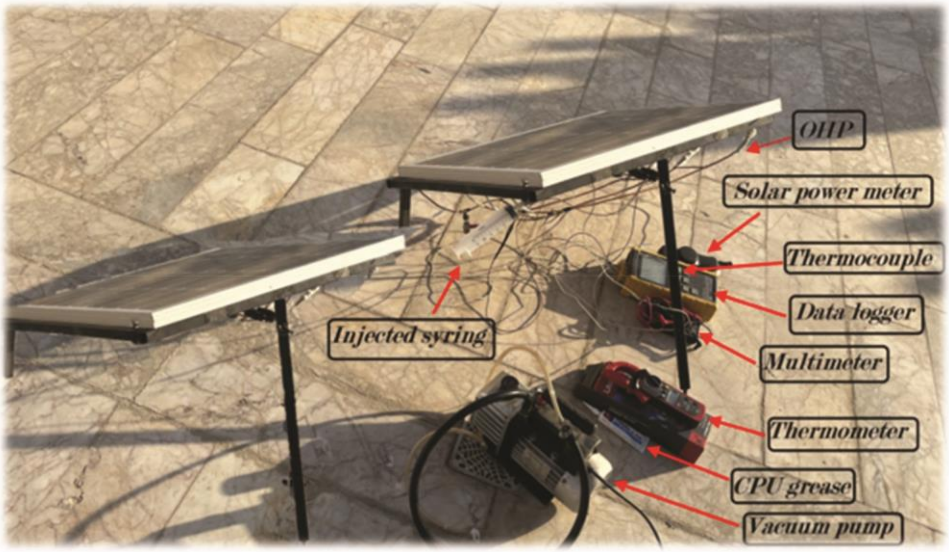

Figure 5. Picture of test bed.

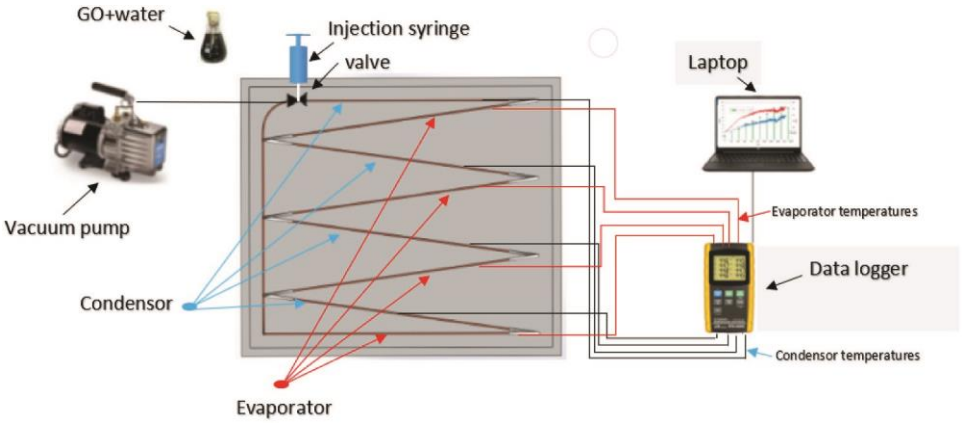

Figure 6. Schematic diagram of experimental layout.

$$T_c = \frac{1}{4}\sum_{i=5}^{8} T_i \tag{2}$$

Thermal resistance (R) is the criterion of $R = \frac{T_e - T_c}{Q}$ (3) assessing OHP performance measured by

Where Q is heat received by OHP (Chen et al. 2020).

Concerning OHP-PV energy analysis, to obtain the thermal efficiency of PV, formula 4 is applied (Alexander et al. 2021).

$$\eta_i = \frac{\dot{m} C_p \int_{t_1}^{t_2} (T_o - T_i)dt}{A \int_{t_1}^{t_2} G dt} \tag{4}$$

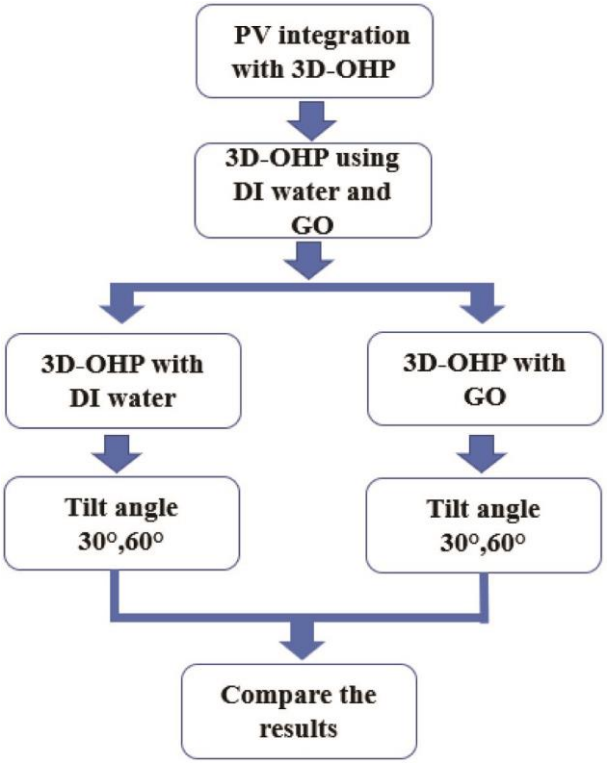

Figure 7. The algorithm of the experiment.

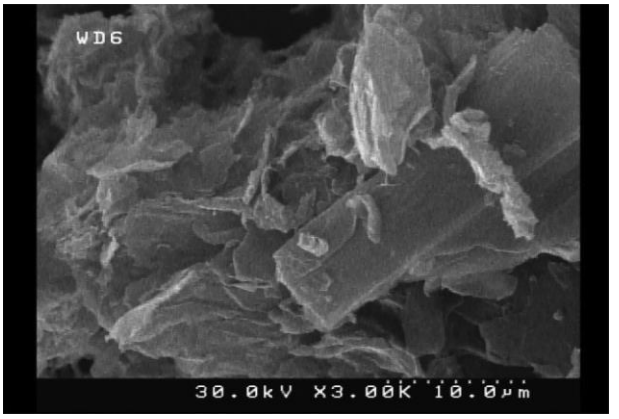

Figure 8. The FESEM image of GO.

PV conversion efficiency is expressed as the portion of electricity generated by PV to input the solar energy, obtained from Equation 5 (Yazdanpanahi, Sarhaddi, and Adeli 2015)

$$\eta_e = \frac{P_{out}}{P_{in}} = \frac{V_{mp} I_{mp}}{AG} \quad (5)$$

where V_{mp} and I_{mp} are peak voltage and current, respectively, A is the area of the PV collector, and G is solar radiation intensity measured by a solar power meter (ST-1307).

Eventually, the improvement of OHP-PV efficiency is calculated by following equation:

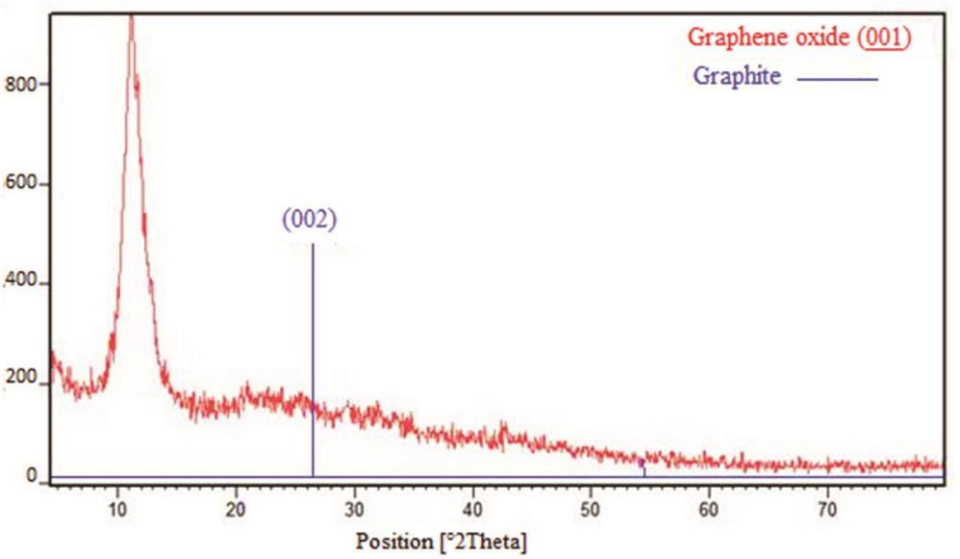

Figure 9. The XRD image of GO.

Table 2. Technical parameters.

Parameters	Values
Thickness	3.4–7 nm
Carbon purity	,99%
Number of layers	Average number of layers 6–10
Surface area (BET)	100–300 m^2=g
Bulk density	0.3g/cc
Lateral dimension	10–50 μm

Table 3. Thermal conductivity (TC) of working fluid.

Working fluid	TC (W/K ·m)
DI/Water	*0.615*
0.2 g/l	0.626

$$\eta_{\mathrm{I}} = \frac{\eta_{\mathrm{OHP-PV}}}{\eta_{\mathrm{PV}}} - 1 \tag{6}$$

Error analysis

This part provides calculations regarding errors connected with measurements.

There are two types of uncertainty (Chandrika et al. 2021). One of them comes from statistical methods which can be calculated by Equation 7, and y hinges on inputs (Agyekum et al. 2021).

$$\mathrm{u(y)} = \sqrt{\left(\frac{\delta\,\mathrm{y}}{\delta \mathrm{w}_1}\right)^2 \mathrm{u}^2(\mathrm{w}_1) + \left(\frac{\delta\,\mathrm{y}}{\delta \mathrm{w}_2}\right)^2 \mathrm{u}^2(\mathrm{w}_2) + \ldots} \tag{7}$$

And another one relates to equipment, which is obtained by (Santbergen et al. 2017).

$$u_n = a_n/\sqrt{3} \tag{8}$$

Where a_n is provided by the manufacturer. The uncertainty of both measuring instruments and measured data is provided in Table 4.

Table 4. Uncertainty values.

Parameter	Uncertainty
Ambient temperature T_a (°C)	±0.12
Condenser temperature T_c (°C)	±0.323
Evaporator temperature T_e (°C)	±0.668
PV cell temperature T_s (°C)	±0.12
Solar radiation intensity I_T (W/m^2)	±1.3
Wind speed Vw (m/s)	±0.13
Voltage V_{oc} (V)	±0.4
current I_{sc} (A)	±0.015

Results and discussion

A series of experiments were performed on the roof with a height of 17 m. During the test period, the PV-T collectors were located at a tilt angle of 30° and 60°, and the experiments were conducted from 7:30 to 17.30. Since PV is a temperature-dependent performance, the PV cell temperature is an imperative parameter that illustrates the effectiveness of the proposed system. The designed OHP-PV model is tested with DI water and graphene oxide nanofluid at a concentration of 0.2 gr/lit.

Climatic parameters

The climatic conditions in Mashhad are more suitable (higher radiation intensity and temperature) over summer period but worse during the winter. In this section, the hourly variation of solar intensity and ambient temperature for experimentation days is provided. The data are demonstrated in Figure 10, which shows the PV temperature during the test time. Also, it is spotted from Figure 11 that the high intensity of solar radiation and surrounding temperature are attributed to the increase in PV cell temperature, and in the mid-day it reaches 1128.5 W/m^2 and 964 W/m^2 when the tilt angle is 30° and 60°, respectively.

Figure 12 demonstrates the average wind speed, varied from over 2 m/s to just under 2.8 m/s during the experiment time. This played a significant role in cooling down the condensers' temperature.

System performance analysis

In this section, analysis is carried out according to data gathered from experiments. Figure 13 displays the thermal resistance of the OHP for water and graphene oxide nanofluid. It can be simply observed that adding graphene oxide contributes to reducing thermal resistance. In higher temperatures, boiling improves, which leads to reduction of thermal resistance of OHP. Using graphene oxide leads to reduce thermal resistance of OHP; nonetheless, with the increase of title angle, thermal resistance experiences a marked reduction and displays more predictable behavior, and as it is expected with increase of title angle, OHP performance improves and thermal resistance decreases.

Generated short- circuit current I_{sc} and open-circuit voltage V_{OC} of PV heavily depend on radiation intensity and PV cell temperature (Hassan et al. 2023); however, when the cell temperature increases, short-circuit current slightly rises but open-circuit voltage experiences considerable reduction as it was displayed in Figure 14. Furthermore, increasing tilt angle gives rise to reduction I_{sc} and V_{OC} since solar radiation is lower at this angle.

According to Figure 15, maximum power follows a downward trend as the temperature rises; nonetheless, the minimum generated power for PV are 35 W and 32.74 W for 30° and 60°, respectively, while the values for OHP-PV when graphene oxide is used as a working fluid (is higher than 37.5 W at 30° and 34.3 W at 60°).

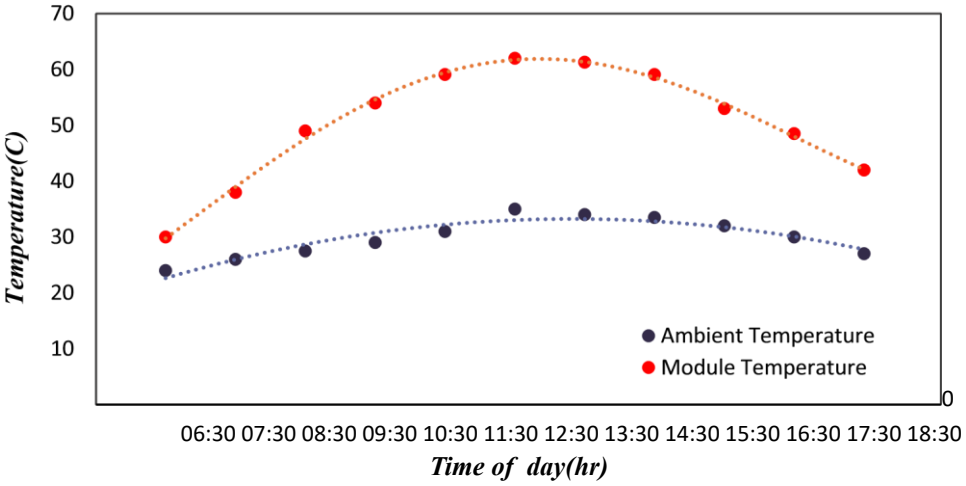

Figure 10. Variation of PV and ambient temperature vs time.

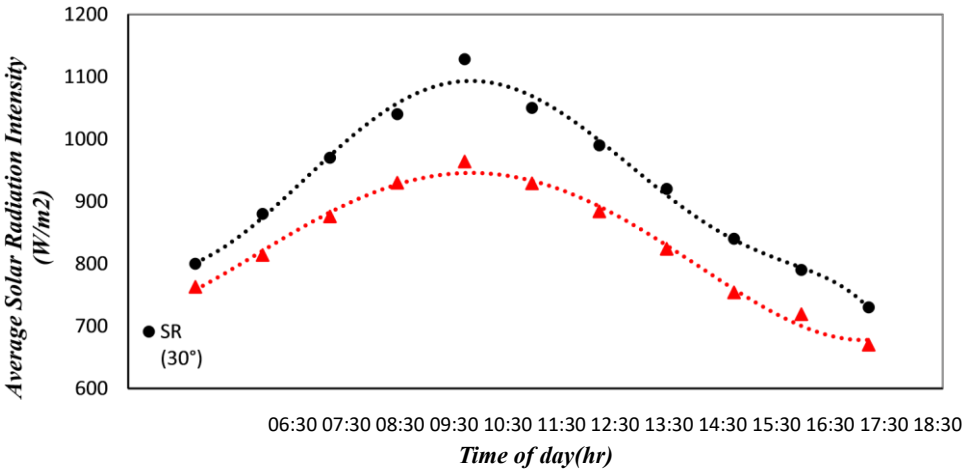

Figure 11. Variation of solar irradiance vs time.

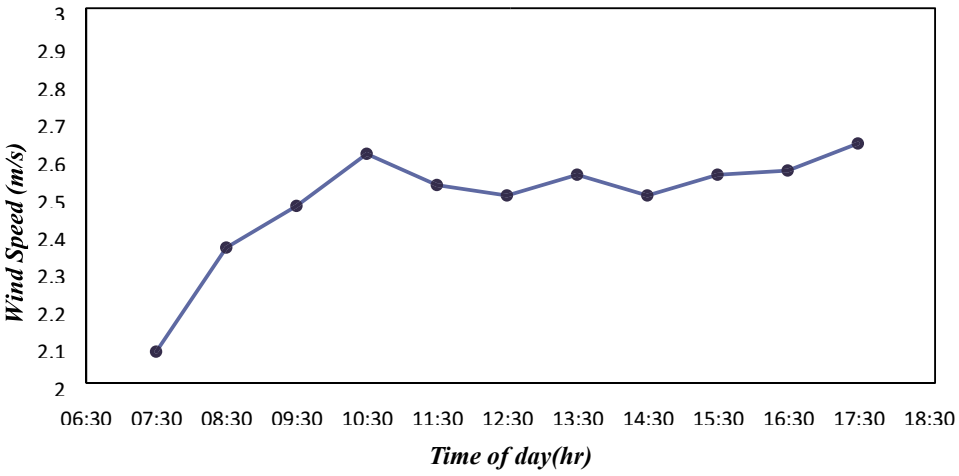

Figure 12. Wind velocity vs time.

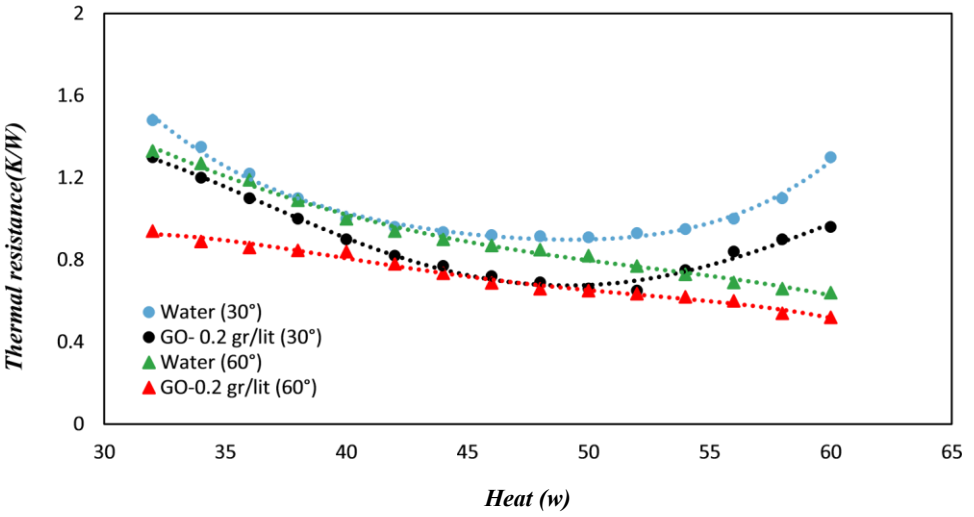

Figure 13. Thermal resistance vs received heat.

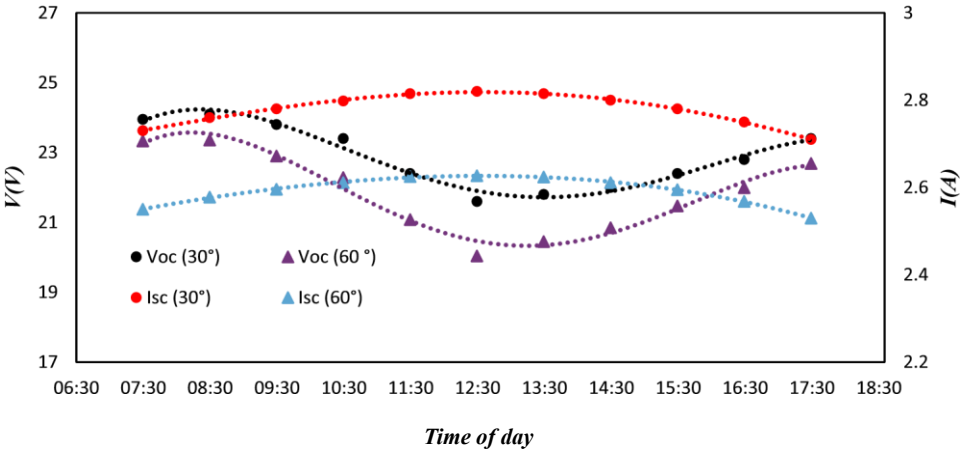

Figure 14. PV temperature effect on V_{OC} and I_{sc} vs time.

Electrical efficiency

The electrical output of the PV system is considered as the total generated electrical power and the total consumed electrical power in operating the mechanical components of the heat dissipation system in the PV module setup, and in the proposed system, there is no external power sources such as pumps and as a result no consumed electrical power.

As it was mentioned earlier, with the increase in PV temperature, the electrical efficiency suffers a decrease, as shown in Figure 16. However, employing OHP causes a remarkable improvement in electrical efficiency, especially at 60° and when it comes to use graphene oxide nanofluid as a coolant, reaching up to 14%.

Figure 17 illustrates the effect of graphene oxide concentration and title angle on the improvement of the electrical efficiency of PV panels. It is clearly observed that the system experiences the highest performance when graphene oxide is used as a working fluid in 60°; however, the PV panel delivers maximum electrical efficiency in 30°.

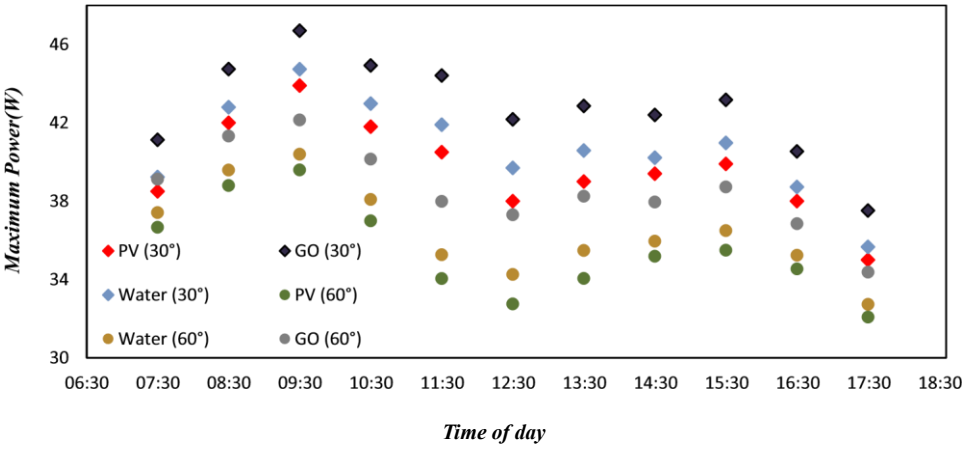

Figure 15. Power output in conventional PV and OHP-PV with different working fluids and angles vs time.

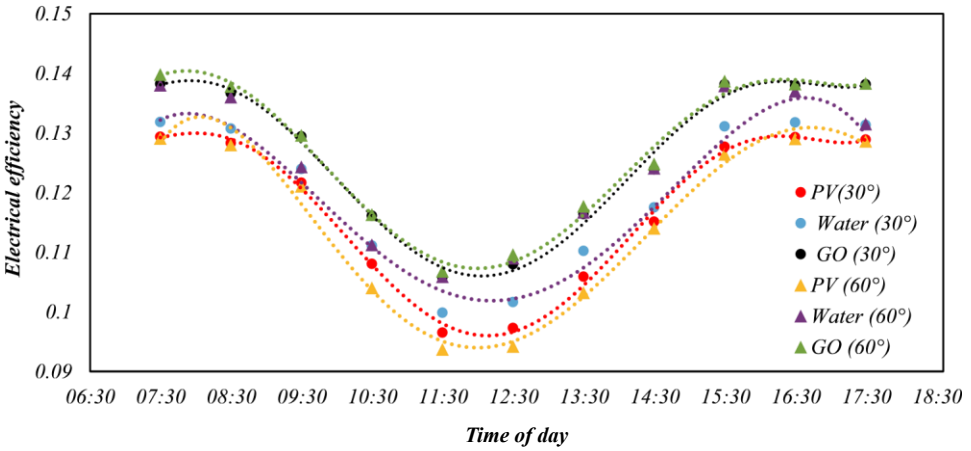

Figure 16. Electrical efficiency in conventional PV and OHP-PV with different working fluids and angle vs time.

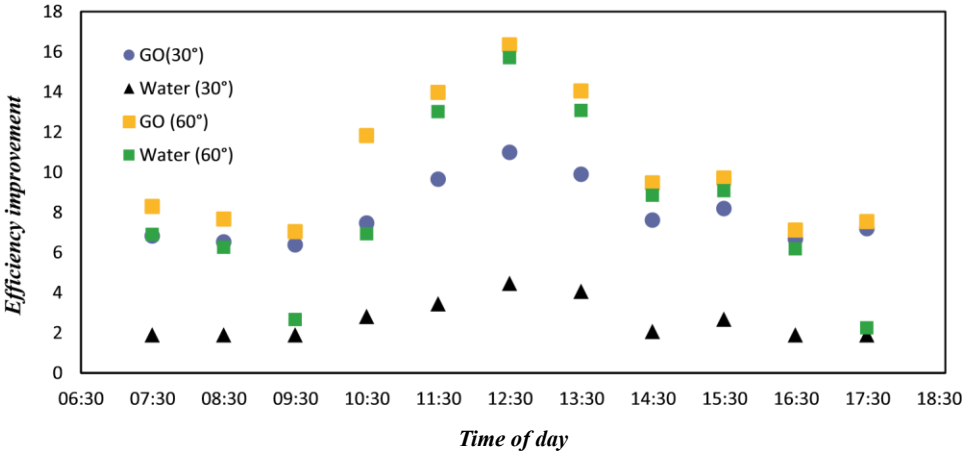

Figure 17. Electrical efficiency improvement with different working fluids and angles vs time.

Conclusions

A PV integrated with a novel 3D-OHP was designed and fabricated in this investigation. Experimental investigations on the efficiency of the proposed system were conducted, and the analyzed results provided in this paper. The photovoltaic power output (PVOUT) is sensitive to the panel temperature and solar irradiance and is reduced by an increase in temperature. In this study, experiments were conducted under the hot climate of Mashhad, and a new cooling method was employed to enhance the electrical efficiency of the photovoltaic panel. For this purpose, the testing rig including a new spiral oscillating heat pipe integrated into PV was constructed and tested with DI water and graphene oxide nanofluid as coolants with a filling ratio of 50% for two different tilt angles. It has been concluded that the proposed cooling system proved highly efficient especially at 60° when GO was used as a coolant, which produced over 16% improvement, while it experienced up to 10% at 30°; however, the efficiency of PV is maximized at 30° due to the fact that the panel is exposed to maximum solar irradiance, which proves the fact that the impact of the tilt angle of PV outweighs the OHP angle. Moreover, using a copper plate is also an innovative idea to facilitate heat exchange between panel and OHP and minimize heat loss. The proposed cooling system is simple and quite cost-effective since it does not require any external power sources such as pumps, which is stimulating factor to be used in industrial and residential rooftop application. Concerning future outlook, although there have been a lot of investigations in this area, PV integrated with HP (especially OHP) have not yet reached the commercialization stage due to the lack of investigation on the long-term performance and durability of OHP-PV systems. It is a requirement for more investigation on the long-term reliability and effectiveness of these systems in real-world applications.

Nomenclature

A	collector aperture area (m^2)
C_p	heat capacity of flowing medium (J/kg k)
G	incident solar radiation (W/m^2)
I	electric current(A)
m _	mass flow rate
Q	heating power (W)
P	power (W)
T	temperature (°C)
R	thermal resistance (°C W^{-1})
V	voltage (V)
η	efficiency (%)
Acronyms	
OHP	oscillating heat pipe
PV	photovoltaic
Subscripts	
c	condenser
e	evaporator
in	input
mp	maximum power point
oc	open-circuit
out	output
sc	short-circuit

References

Afsari, K., M. R. S. Emami, S. Zahmatkesh, J. J. Klemeš, and A. Bokhari. 2023. Optimizing the thermal performance of the thermosyphon heat pipe for energy saving with graphene oxide nanofluid. *Energy* 274:127422. doi:10.1016/j.energy.2023.127422 .

Agyekum, E. B., S. PraveenKumar, N. T. Alwan, V. I. Velkin, S. E. Shcheklein, and S. J. Yaqoob. 2021. Experimental investigation of the effect of a combination of active and passive cooling mechanism on the thermal characteristics and efficiency of solar PV module. *Inventions* 6 (4):63. doi:10.3390/inventions6040063 .

Ahmadian-Elmi, M., M. R. Hajmohammadi, S. S. Nourazar, K. Vafai, and M. B. Shafii. 2023. Effect of filling ratio, number of loops, and transverse distance on the performance of pulsating heat pipe in a microchannel heat sink. *Numerical Heat Transfer, Part A: Applications* 85 (8):1278–99. doi:10.1080/10407782.2023.2200217 .

Alexander, K., S. S. Gajghate, A. S. Katarkar, A. Majumder, and S. Bhaumik. 2021. Role of nanomaterials and surfactants for the preparation of graphene nanofluid: A review. Materials Today: Proceedings, vol. 44, 1136–43. doi:10.1016/j.matpr.2020.11.231 .

Ali, H. M. 2020. Recent advancements in PV cooling and efficiency enhancement integrating phase change materials based systems–A comprehensive review. *Solar Energy* 197:163–98. doi:10.1016/j.solener.2019.11.075 .

Alizadeh Jajarm, A. R., H. R. Goshayeshi, and K. Bashirnezhad. 2022. Experimental study of thermal performance of a newly designed pulsating heat pipe with Fe3O4 nanofluid-exposed magnetic field and corrugated evaporator. *International Journal of Thermophysics* 43 (3):40. doi:10.1007/s10765-021-02971-1 .

Allouhi, A., and M. Benzakour Amine. 2021. Heat pipe flat plate solar collectors operating with nanofluids. *Solar Energy Materials & Solar Cells* 219:110798. doi:10.1016/j.solmat.2020.110798 .

Alqahtani, A. A., S. Edwardson, M. Marengo, and V. Bertola. 2022. Performance of flat-plate, flexible polymeric pulsating heat pipes at different bending angles. *Applied Thermal Engineering* 216:118948. doi:10.1016/j.applthermaleng.2022.118948 .

Alshukri, M. J., A. K. Hussein, A. A. Eidan, and A. I. Alsabery. 2022. A review on applications and techniques of improving the performance of heat pipe-solar collector systems. *Solar Energy* 236:417–33. doi:10.1016/j.solener.2022.03.022 .

Aste, N., F. Leonforte, and C. Del Pero. 2015. Design, modeling and performance monitoring of a photovoltaic–thermal (PVT) water collector. *Solar Energy* 112:85–99. doi:10.1016/j.solener.2014.11.025 .

Browne, M. C., B. Norton, and S. J. McCormack. 2016. Heat retention of a photovoltaic/thermal collector with PCM. *Solar Energy* 133:533–48. doi:10.1016/j.solener.2016.04.024 .

Chandrika, V. S., A. Karthick, N. M. Kumar, P. M. Kumar, B. Stalin, and M. Ravichandran. 2021. Experimental analysis of solar concrete collector for residential buildings. *International Journal of Green Energy* 18 (6):615–23. doi:10.1080/15435075.2021.1875468 .

Chen, F., M. Hu, A. Badiei, M. Yu, Z. Huang, Z. Wang, and X. Zhao. 2020. Experimental and numerical investigation of a novel photovoltaic/thermal system using micro-channel flat loop heat pipe (PV/T-MCFLHP). *International Journal of Low-Carbon Technologies* 15 (4):513–27. doi:10.1093/ijlct/ctaa019 .

Coldrick, K., J. Walshe, S. J. McCormack, J. Doran, and G. Amarandei. 2023a. Experimental and theoretical evaluation of a commercial luminescent dye for PVT systems. *Energies* 16 (17):6294. doi:10.3390/en16176294 .

Coldrick, K., J. Walshe, S. J. McCormack, J. Doran, and G. Amarandei. 2023b. The role of solar spectral beam splitters in enhancing the solar-energy conversion of existing PV and PVT technologies. *Energies* 16 (19):6841. doi:10.3390/en16196841 .

Dai, Y., R. Zhang, Z. Qin, K. Liu, C. Liu, and J. Zhao. 2024. Research on the thermal performance and stability of three-dimensional array pulsating heat pipe for active/passive coupled thermal management application. *Applied Thermal Engineering* 245:122793. doi:10.1016/j.applthermaleng.2024.122793 .

Divitini, G., S. Cacovich, F. Matteocci, L. Cinà, A. Di Carlo, and C. Ducati. 2016. In situ observation of heat-induced degradation of perovskite solar cells. *Nature Energy* 1 (2):1–6. doi:10.1038/nenergy.2015.12 .

Gyamfi, B. A., P. A. Kwakwa, and T. S. Adebayo. 2023. Energy intensity among European Union countries: The role of renewable energy, income and trade. *International Journal of Energy Sector Management* 17 (4):801–19. doi:10.1108/ IJESM-05-2022-0018 .

Hasan, H. A., J. S. Sherza, J. M. Mahdi, H. Togun, A. M. Abed, R. K. Ibrahim, and W. Yaïci. 2022. Experimental evaluation of the thermoelectrical performance of photovoltaic-thermal systems with a water-cooled heat sink. *Sustainability* 14 (16):10231. doi:10.3390/su141610231 .

Hassan, A., S. Abbas, S. Yousuf, F. Abbas, N. M. Amin, S. Ali, and M. S. Mastoi. 2023. An experimental and numerical study on the impact of various parameters in improving the heat transfer performance characteristics of a water based photovoltaic thermal system. *Renewable Energy* 202:499–512. doi:10.1016/j.renene.2022.11.087 .

He, Y., D. Jiao, G. Pei, X. Hu, and L. He. 2020. Experimental study on a three-dimensional pulsating heat pipe with tandem tapered nozzles. *Experimental Thermal and Fluid Science* 119:110201. doi:10.1016/j.expthermflusci.2020.110201 .

Huang, P., Y. Li, G. Yang, Z. X. Li, Y. Q. Li, N. Hu, and S.-Y. Fu, K. S. Novoselov. 2021. Graphene film for thermal management: A review. *Nano Materials Science* 3 (1):1–16. doi:10.1016/j.nanoms.2020.09.001 .

Jose, J., and T. K. Hotta. 2023. A comprehensive review of heat pipe: Its types, incorporation techniques, methods of analysis and applications. *Thermal Science and Engineering Progress* 101860:101860. doi:10.1016/j.tsep.2023.101860 .

Kargaran, M., H. R. Goshayeshi, H. Pourpasha, I. Chaer, and S. Z. Heris. 2022. An extensive review on the latest developments of using oscillating heat pipe on cooling of photovoltaic thermal system. *Thermal Science and Engineering Progress* 36:101489. doi:10.1016/j.tsep.2022.101489 .

Kaya, M., A. Etem Gürel, Ü. Ağbulut, İ. Ceylan, S. Çelik, A. Ergün, and B. Acar. 2019. Performance analysis of using CuO-Methanol nanofluid in a hybrid system with concentrated air collector and vacuum tube heat pipe. *Energy Conversion and Management* 199:111936. doi:10.1016/j.enconman.2019.111936 .

Lan, H. H. 2020. *The manufacturing of a large-scale pulsating heat pipe and its heat transfer performance [D]*. North China Electric Power University.

Li, G., T. M. Diallo, Y. G. Akhlaghi, S. Shittu, X. Zhao, X. Ma, and Y. Wang. 2019. Simulation and experiment on thermal performance of a micro-channel heat pipe under different evaporator temperatures and tilt angles. *Energy* 179:549–57. doi:10.1016/j.energy.2019.05.040 .

Li, M., L. Li, and D. Xu. 2019. Effect of filling ratio and orientation on the performance of a multiple turns helium pulsating heat pipe. *Cryogenics* 100:62–68. doi:10.1016/j.cryogenics.2019.04.006 .

Li, S., H. Pei, D. Liu, Y. Shen, X. Tao, and Z. Gan. 2023. Visualization study on the flow characteristics of a nitrogen pulsating heat pipe. *International Communications in Heat and Mass Transfer* 143:106722. doi:10.1016/j.icheatmasstransfer.2023.106722 .

Li, H., J. Ren, D. Yin, G. Lu, C. Du, X. Jin, and Y. Jia. 2022. Effects of inclination angle and heat power on heat transfer behavior of flat heat pipe with bionic grading microchannels. *Applied Thermal Engineering* 206:118079. doi:10.1016/j. applthermaleng.2022.118079 .

Liu, X., L. Xu, C. Wang, and X. Han. 2019. Experimental study on thermo-hydrodynamic characteristics in a micro oscillating heat pipe. *Experimental Thermal and Fluid Science* 109:109871. doi:10.1016/j.expthermflusci.2019.109871.

Natsume, K., T. Mito, N. Yanagi, H. Tamura, T. Tamada, K. Shikimachi, and N. Hirano, S. Nagaya. 2011. Heat transfer performance of cryogenic oscillating heat pipes for effective cooling of superconducting magnets. *Cryogenics* 51 (6):309–14. doi:10.1016/j.cryogenics.2010.07.001 .

Nazari, M. A., R. Ghasempour, M. H. Ahmadi, G. Heydarian, and M. B. Shafii. 2018. Experimental investigation of graphene oxide nanofluid on heat transfer enhancement of pulsating heat pipe. *International Communications in Heat and Mass Transfer* 91:90–94. doi:10.1016/j.icheatmasstransfer.2017.12.006 .

Novoselov, K. S., P. Blake, and M. I. Katsnelson. 2008. Graphene: Electronic properties. 1–6.

Omri, M., F. Selimefendigil, H. T. Smaoui, and L. Kolsi. 2022. Cooling system design for photovoltaic thermal management by using multiple porous deflectors and nanofluid. *Case Studies in Thermal Engineering* 39:102405. doi:10.1016/j.csite.2022.102405 .

Pagliarini, L., N. Iwata, and F. Bozzoli. 2023. Pulsating heat pipes: Critical review on different experimental techniques. *Experimental Thermal and Fluid Science* 148:110980. doi:10.1016/j.expthermflusci.2023.110980 .

Qian, N., F. Jiang, M. Marengo, Y. Fu, and J. Xu. 2023. Thermal performance of a radial-rotating oscillating heat pipe and its application in grinding processes with enhanced heat transfer. *Applied Thermal Engineering* 233:121213. doi:10.1016/j.applthermaleng.2023.121213 .

Qu, J., J. T. Zhao, and Z. H. Rao. 2017. Experimental investigation on thermal performance of multi-layers three-dimensional oscillating heat pipes. *International Journal of Heat and Mass Stansfer* 115:810–19. doi:10.1016/j.ijheatmasstransfer.2017.08.082 .

Razali, S. N., A. Ibrahim, A. Fazlizan, M. F. Fauzan, R. K. Ajeel, E. Z. Ahmad, and W. E. Ewe, H. A. Kazem. 2023. Performance enhancement of photovoltaic modules with passive cooling multidirectional tapered fin heat sinks (MTFHS). *Case Studies in Thermal Engineering* 50:103400. doi:10.1016/j.csite.2023.103400 .

Rittidech, S., A. Donmaung, and K. Kumsombut. 2009. Experimental study of the performance of a circular tube solar collector with closed-loop oscillating heat-pipe with check valve (CLOHP/CV. *Renewable Energy* 34 (10):2234–38. doi:10.1016/j.renene.2009.03.021 .

Rouhani, A., M. Abdollahpour, M. Golzarian, and H. Abutorabi Zarchi. 2017. Optimal angle for solar panels to receive maximum radiation: case of mashhad city. *Iranian Journal of Energy* 20 (2):103–25.

Sadeghinezhad, E., M. Mehrali, R. Saidur, M. Mehrali, S. T. Latibari, A. R. Akhiani, and H. S. C. Metselaar. 2016. A comprehensive review on graphene nanofluids: Recent research, development and applications. *Energy Conversion and Management* 111:466–87. doi:10.1016/j.enconman.2016.01.004 .

Salarnia, M., D. Toghraie, M. A. Fazilati, B. Mehmandoust, and M. Pirmoradian. 2023. The effects of different nanoparticles on physical and thermal properties of water in a copper oscillating heat pipe via molecular dynamics simulation. *Journal of the Taiwan Institute of Chemical Engineers* 143:104721. doi:10.1016/j.jtice.2023.104721 .

Santbergen, R., V. A. Muthukumar, R. M. E. Valckenborg, W. J. A. van de Wall, A. H. M. Smets, and M. Zeman. 2017. Calculation of irradiance distribution on PV modules by combining sky and sensitivity maps. *Solar Energy* 150:49–54. doi:10.1016/j.solener.2017.04.036 .

Su, Z., Y. Hu, S. Zheng, T. Wu, K. Liu, M. Zhu, and J. Huang. 2022. Recent advances in visualization of pulsating heat pipes: A review. *Applied Thermal Engineering* 221:119867. doi:10.1016/j.applthermaleng.2022.119867 .

Tawfik, M. M. 2017. Experimental studies of nanofluid thermal conductivity enhancement and applications: A review. *Renewable and Sustainable Energy Reviews* 75:1239–53. doi:10.1016/j.rser.2016.11.111 .

Tiwari, A. K., K. Chatterjee, S. Agrawal, and G. K. Singh. 2023. A comprehensive review of photovoltaic-thermal (PVT) technology: Performance evaluation and contemporary development. *Energy Reports* 10:2655–79. doi:10.1016/j.egyr. 2023.09.043 .

Wang, X., Q. Wen, J. Yang, J. Xiang, Z. Wang, C. Weng, and F. Chen, S. Zheng. 2022. A review on data centre cooling system using heat pipe technology. *Sustainable Computing: Informatics and Systems* 35:100774. doi:10.1016/j.suscom.2022.100774.

Wang, G., Y. Yang, W. Yu, T. Wang, and T. Zhu. 2022. Performance of an air-cooled photovoltaic/thermal system using micro heat pipe array. *Applied Thermal Engineering* 217:119184. doi:10.1016/j.applthermaleng.2022.119184 .

Yazdanpanahi, J., F. Sarhaddi, and M. M. Adeli. 2015. Experimental investigation of exergy efficiency of a solar photovoltaic thermal (PVT) water collector based on exergy losses. *Solar Energy* 118:197–208. doi:10.1016/j.solener.2015.04.038 .

Zamanifard, A., M. Muneeshwaran, Y. H. Wang, and C. C. Wang. 2023. A novel 3-D pulsating heat pipe module for high heat-flux applications. *Applied Thermal Engineering* 228:120549. doi:10.1016/j.applthermaleng.2023.120549 .

Zhan, J., X. Chen, Y. Ji, P. Zheng, and W. Duan. 2023. Experimental study of ethane pulsating heat pipe with varying evaporator lengths based on pulse tube refrigerator. *International Journal of Refrigeration* 145:40–49. doi:10.1016/j.ijrefrig.2022.09.010 .

Zhang, Q., S. He, T. Song, M. Wang, Z. Liu, J. Zhao, and Y. Shi, X. Huang, K. Han, J. Qi. 2023. Modeling of a PV system by a back-mounted spray cooling section for performance improvement. *Applied Energy* 332:120532. doi:10.1016/j.apenergy.2022.120532.